Redoxless electrochemical capacitance spectroscopy for investigating surfactant adsorption on screen-printed carbon electrodes

Tzong-Jih Cheng*, Hsien-Yi Hsiao, Pei-Chia, Tsai, Richie L. C. Chen

Department of Biomechatronics Engineering, College of Bio-Resources and Agriculture, National Taiwan University, Taipei, Taiwan

*Corresponding authors: *E-mail:* tzongjih@ntu.edu.tw (Tzong-Jih Cheng)

S1. Simulation—complex impedance and capacitance of an equivalent circuit with parallel R_{ct} and various capacitance C_{dl}

The EIS of an electrode–electrolyte interface can be represented by an equivalent circuit involving some electronic elements. Typical equivalent circuits in electrochemical measurements are shown in Fig. 1. The simplest equivalent circuit for simulating an ideal-polarization electrode with the non-Faradaic process, mimicking perfect insulation on the surface, is dielectric layer capacitance C_m in series with solution resistance R_s (Fig. 1(c)). As the charge transfer resistance R_{ct} is assumed to be necessary for the electrode with the Faradaic process, mimicking imperfect insulation on the surface, the equivalent circuit involves R_m and C_m in parallel (Fig. 1(b)). Similarly, R_{ct} and C_{dl} in parallel were used as a conventional equivalent model of uncoated or lightly coated electrodes (Fig. 1(a)). In this study, the parallel resistance (R_m or R_{ct}) and capacitance (C_m or C_{dl}) were combined to obtain a simple model of the interface, but the solution resistance was omitted ($R_s = 0\ \Omega$) in the simulations. In the analysis of electrochemical impedance data, every element was calculated by fitting a curve to experimental results on the basis of the equivalent circuit. Therefore, knowing the details of the relationship between the equivalent circuit and impedance loci is necessary.

The calculated results of EIS for a constant R_{ct} in parallel with various-value C_{dl} are presented in Fig. S1(a). The Nyquist impedance plot shows the locus of a semi-circle at a complex impedance plane. The impedance converges at the origin and at R_{ct} in high- and low-frequency ranges, respectively. Different values of C_{dl} were discovered to result in identical patterns of Nyquist capacitance plot loci. Because the time constant of dielectric relaxation ($\tau = 1/\omega = 1/2\pi f = R_{ct}C_{dl}$) could be obtained from the peak of the semi-circle locus, $R_{ct}C_{dl}$ could be obtained from the frequency f at the maximum of the imaginary part ($R_{ct}C_{dl} = 1/2\pi f$) and C_{dl} could be calculated from the values of $R_{ct}C_{dl}$ and R_{ct}. In Fig. 2(a), the shape of the impedance spectrum is unaffected by C_{dl}. The frequency f at the maximum of the imaginary part of the semi-circle locus decreases but the time constant of dielectric relaxation increases with an increase in C_{dl}. This result implies that the interfacial capacitance C_{dl} could not be intuitively determined from the EIS loci; additional calculations were necessary.

The complex capacitance in the case of parallel R_{ct} and C_{dl} is expressed as follows: $C' = C_{dl}$; $C'' = -1/\omega R_{ct}$. The calculated results for the complex capacitance given various C_{dl} values are illustrated in Fig. S1(b). The complex capacitance describes the locus in parallel with the imaginary axis on the complex plane and converges at C_{dl} on the real axis in the high-frequency range. Contrary to the EIS in Fig. S1(a), the value of C_{dl} could be obtained directly from converged points on the

real axis in Fig. S1(b). The results of this work in a wider range (1 nF–10 μF) of parallel capacitance C_{dl} are consistent with those of a previous study [18] in which a small capacitance variation (10–30 μF) was investigated.

Complex impedances in the EIS Nyquist plot show the complete loci of semi-circles and converged points on the real axis except under the condition of a long time constant $\tau = 0.1$ (R_{ct} = 1 MΩ, C_{dl} = 10 μF). By contrast, complex capacitances in the ECS Nyquist plot exhibit vertical lines and converged points on the real axis for all time constants (τ = 0.1–0.00001). The intercept points of the real axis in the complex impedance and capacitance intuitively present the R_{ct} (or R_m) and C_{dl} (or C_m) of the EIS (Z-domain) and ECS (C-domain) Nyquist plot, respectively.

These simulation results indicate that various capacitances parallel with a fixed resistance could be intuitively distinguished using the ECS Nyquist plots with no additional calculations being required, which was not the case for EIS.

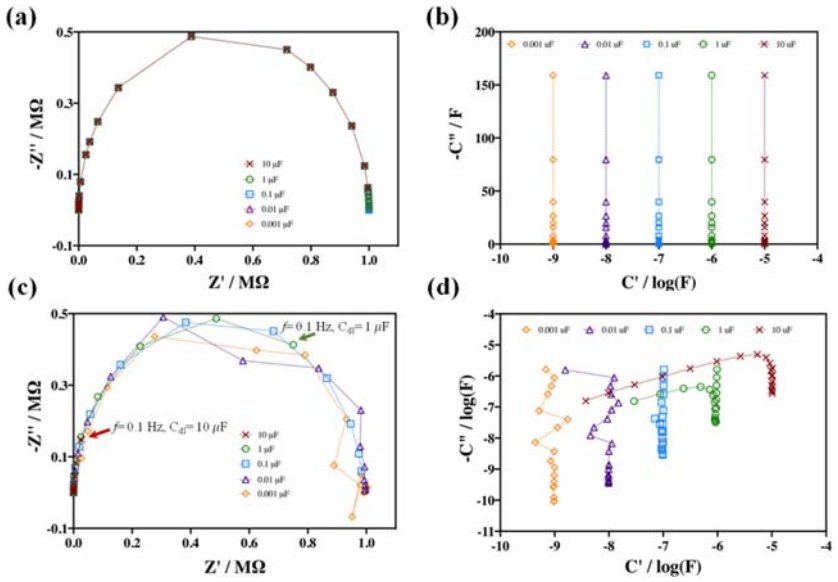

Figure S1. Simulation and experimental validation by using dummy cells. (a) Calculated results of electrochemical impedance of a parallel circuit consisting of R_{ct} (R_m) and C_{dl} (C_m) modeled as illustrated in Fig. 1(b) and 1(c). R_s= 0 Ω; R_{ct}= 1 MΩ; ×: C_{dl}= 1.0 × 10^{-5} F; ○: C_{dl}= 2.0 × 10^{-6} F; □: C_{dl}= 3.0 × 10^{-7} F; ▽: C_{dl}= 3.0 × 10^{-8} F; ◇: C_{dl}= 3.0 × 10^{-9} F. (b) Complex capacitances calculated from (a). (c) EIS impedance plots of electronic dummy cells . Rs= 100 Ω; values of R_{ct} (R_m) and C_{dl} (C_m) are same as in (a) . (d) Complex capacitances (ECS) calculated from (c). Rs= 100 Ω; values of C_{dl} (C_m) and R_{ct} (R_m) are same as in (a). The frequency range of (b) is 0.2 Hz−10 kHz.

S2. EIS and ECS of equivalent circuits verification by electronic dummy cells

The electronic dummy cell, which is constructed using solid electronic parts (resistors and capacitors), is a common technique in the modeling of electrochemical systems used in experiments. In this study, such a cell was used to mimic interfacial impedance and potentiostatic EIS. Various combinations of R_{ct} in parallel with C_{dl} and then in series with a fixed R_s for electronic dummy cells consistent with simulations (Fig. S1(a)) are a useful means of verifying the effectiveness of models by conducting electrochemistry experiments.

The results of EIS (Z^*) and ECS (C^*) for various values of C_{dl} are displayed in Fig. S1(c) and S1(d), respectively. The complex impedance function $Z^*(\omega)$ is convertible into the complex capacitance $C^*(\omega)$ through the expression $C^*(\omega) = 1/j\omega Z^*(\omega)$. Practically, this involves taking the data resolved through a standard impedance analysis ($Z^*(\omega)$), sampled across a range of frequencies at any steady state potential, and converting them phasorially into $C^*(\omega)$ with real and imaginary components. When processing $Z^*(\omega)$ data sets in this manner, the imaginary part of the capacitance can be obtained by noting that $C'' = \varphi Z'$ and $C' = \varphi Z''$, where $\varphi = (2\omega|Z|)^{-1}$ and $|Z|$ is the modulus of Z^*.

The experimental EIS Nyquist impedance plots (Fig. 2(c)) also describe similar loci of semi-circles on the complex plane to those in the simulations (Fig. S1 (a)). Complete semi-circle loci were obtained for a short time constant of $\tau \leq 0.1$ (C_{dl} = 0.1, 0.01, and 0.001 μF). However, the Nyquist impedance plots show only slightly-larger-than-quarter-circle and limited arc loci (arrow indicators in Fig. S1(b)) for τ = 1 (C_{dl} = 1 μF) and τ = 10 (C_{dl} = 10 μF), respectively. A favorable fit to the typical semi-circle pattern was obtained only under the condition of τ = 0.1 (R_{ct} = 1 MΩ, C_{dl} = 1 μF); a considerable variation was obtained in the lower-frequency range for $\tau \leq$ 0.01. In an EIS Nyquist plot, the intercept of the real axis is conventionally used to quantify R_{ct}, and the frequency *f* at the maximum of the imaginary part is occasionally used to determine C_{dl}. The results of this study indicate that a fine and complete locus of a semi-circle in the EIS Nyquist plot for determining R_{ct} could be obtained for approximately τ = 0.1, but an incomplete semi-circle pattern was obtained for $\tau \geq$ 1 and poor fitness for $\tau \leq 0.01$. Furthermore, C_{dl} could be effectively calculated from the complex impedance under $\tau \leq$ 1 because the locus of the Nyquist plot had a maximum of the imaginary part at the quarter of the circle locus.

The complex capacitance calculated from the complex impedance Nyquist plots is illustrated in Fig. S1(d). The $\log_{10}$ scale at the real axis is presented to enable a comparison with the simulation results shown in Fig. S1(b). The vertical line parts of all loci of complex capacitances and intercept points of the extended vertical lines at the real axis are consistent with the simulation results shown in Fig. 2(b), as well as

the nominal values of capacitors used in the electronic dummies. In the ECS Nyquist capacitance plot, the real-axis intercept of the extended vertical line part is a useful indicator of C_{dl} or C_m. The typical locus of complex capacitance is a combination of a complete semi-circle and a vertical line (not shown) as $\tau \geq 1$. The integrity of semi-circle loci gradually decreases as τ decreases. Fortunately, an intuitive determination of C_{dl} is dependent only on the vertical line part and independent of the pattern integrity of the semi-circle in the ECS Nyquist capacitance plot.

Further model verification by using electronic dummies with a constant C_{dl}/C_m in parallel with various R_{ct} is shown in Fig. 2. The integrity of semi-circle loci and consistency of vertical lines in the C-domain (ECS Nyquist capacitance plots) were discovered under all conditions (Fig. 2(b)) but were found only for $\tau \leq 0.1$ in the Z-domain (ECS Nyquist impedance plots; Fig. 2(a)). The slight inconsistency in C_{dl} determined through ECS Nyquist capacitance plots may have been due to the 10% tolerance of commercial capacitor parts used in dummy cells. A high interfacial resistance (R_{ct} or R_m = 1 or 10 MΩ) affects the integrity and imaginary value of the semi-circle patterns of Nyquist plot loci in EIS and ECS, respectively. In the ECS plots (Fig. 2(b), 2(d), and 2(f)), the shapes of the integrity of the semi-circle loci were not negatively affected by smaller resistances ($R_{ct} \leq 0.1$ MΩ) but only by the magnitude of imaginary capacitance values (C”), which are noncritical for quantitative analysis. However, these results indicate that EIS is a useful and intuitive approach for determining lower interfacial resistance but useless for investigating higher interfacial resistance ($R_{ct} \geq 1$ MΩ). The redox couples used in conventional EIS enforce the working condition of low interfacial resistance, which results in a complete semi-circle pattern in Nyquist impedance plots. As is well known, EIS, dominated by the Faradaic process, is mainly used for the analysis of low- resistive solid–liquid interfaces, but its ability to resolve highly resistive interfaces is rather limited. Furthermore, ECS is a useful and intuitive approach for determining C_{dl} or C_m under all conditions despite a high-resistance interface. The present results indicate that ECS can be complementary to EIS in investigating interfaces with highly resistive interfaces and imply that a redox couple is not necessarily required to explore solid–liquid interfaces because the interfacial capacitance is an effective and sufficient parameter. This implicit potential is fully explored in the following subsections.

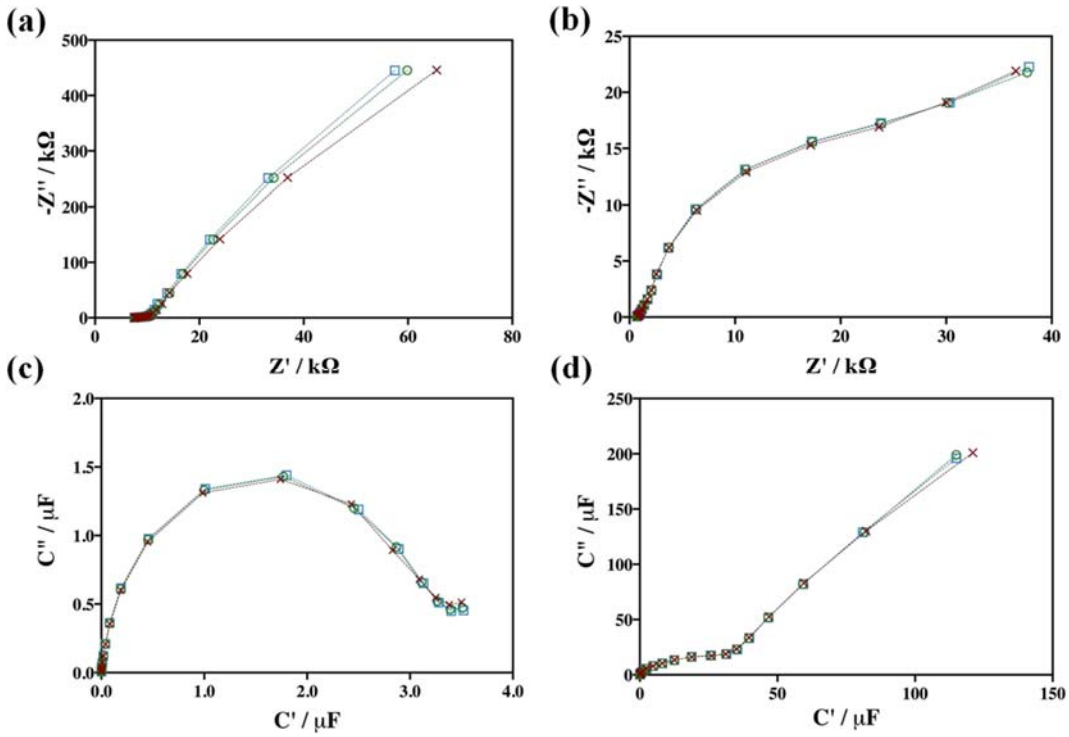

Figure S2. Redoxless EIS and ECS of SDS/SPCE. (a) Redoxless EIS Nyquist plots (area = 0.45 mm^2); (b) redox EIS Nyquist plots; (c) redoxless ECS capacitance plots calculated from (a); (d) redox ECS capacitance plots calculated from (b). Redoxless EIS was performed at the bias +0.0 V vs. Ag/AgCl in 0.1 M PBS (pH7.0); redox EIS was conducted at the bias +0.3 V in the presence of 10 mM $[Fe(CN)_6]^{3-/4-}$ in PBS. The AC frequencies for EIS experiments ranged from 10 kHz to 0.1 Hz with an amplitude of 10 mV. N=3.

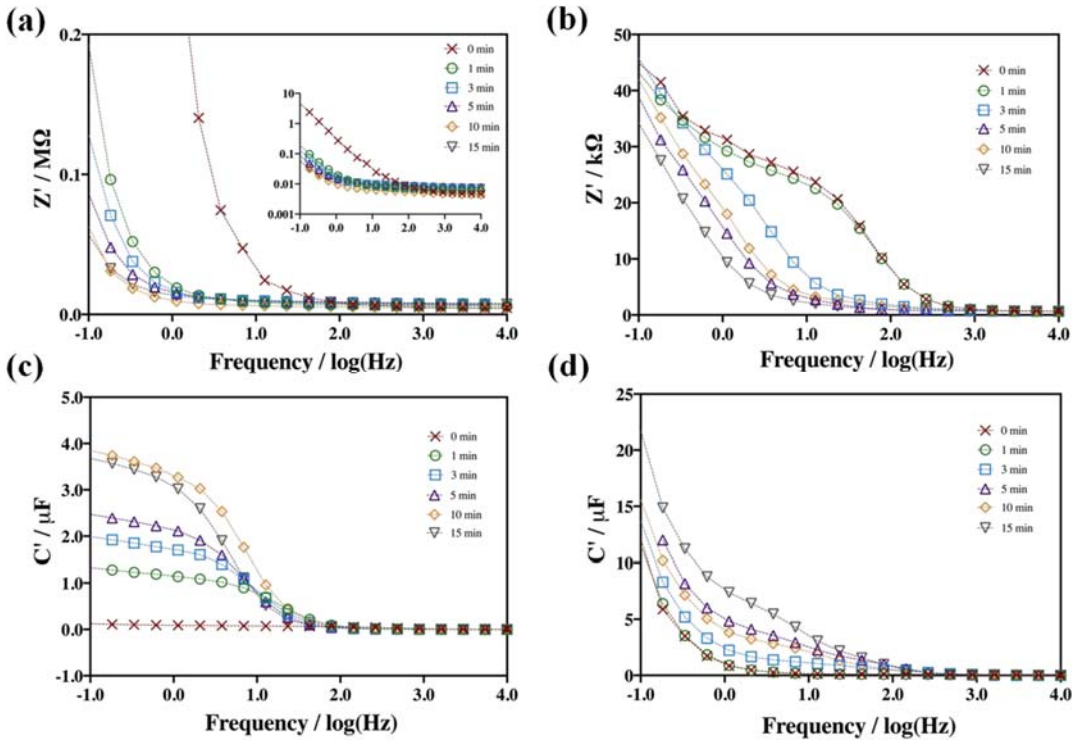

Figure S3. Bode resistance and capacitance plots of SDS/SPCE under various incubation times for SDS adsorption. (a) Redoxless EIS Bode resistance plots (area= 0.45 mm^2); (b) redox EIS Bode resistance plots; (c) redoxless ECS Bode capacitance plots; (d) redox ECS Bode capacitance plots. Redoxless EIS was performed at the bias +0.0 V vs. Ag/AgCl in 0.1 M PBS (pH7.0); redox EIS was conducted at the bias +0.3 V in the presence of 10 mM $[Fe(CN)_6]^{3-/4-}$ in PBS. The AC frequencies for EIS experiments ranged from 10 kHz to 0.1 Hz with an amplitude of 10 mV.